FAR-INFRARED REFLECTION SPECTRA OF MONOCLINIC ZnP_2

Osamu ARIMOTO, Mitsuru SUGISAKI, Masaru EGUCHI,
Makoto WATANABE,* and Kaizo NAKAMURA

Department of Physics, Okayama University, Okayama 700
**Institute for Molecular Science, Okazaki 404*

Monoclinic zinc diphosphide (β-ZnP_2) shows a very clear hydrogen-like exciton series near the fundamental absorption edge. Recently we have observed two closely separated resonant Raman (RR) lines with energies of 260 and 252 cm^{-1} under excitation into the exciton resonance region at 2 K.[1] From comparison with the infrared reflection spectra at room temperature (RT),[2] they are tentatively assigned to be due to the scattering of exciton polaritons by the longitudinal optical (LO) phonons with those energies. However, there is no data of infrared spectra at low temperatures. The unit cell of β-ZnP_2 contains 8 zinc atoms and 16 phosphorous atoms, giving rise to 72 phonon branches. Of these, 33 modes are infrared-active and 36 modes are Raman-active.

In the present study, we have measured far-infrared reflection spectra of β-ZnP_2 at temperatures 300, 80, and 10 K. Experiments were performed at the beam line BL6A. A Si-disk was used as the beam splitter of the interferometer, by which the spectral region is extended up to ~ 300 cm^{-1}. Figure 1 shows reflection spectrum (solid curve) for the *E//b* polarization at RT. Two prominent reflection bands labelled A and B of the B_u mode are seen, whose reflection peaks locate at 214 and 245 cm^{-1}. For the *E//c* polarization, one reflection band of the A_u mode is observed at 228 cm^{-1}. The broken curve shows the calculated spectrum obtained by using a many-oscillator model, in which the dispersion of the complex dielectric constant is given by the expression

$$\varepsilon(\omega) = \varepsilon_1(\omega) + i\varepsilon_2(\omega) = \varepsilon_\infty + \sum_j \frac{\varepsilon_\infty(\omega_{Lj}^2 - \omega_{Tj}^2)}{\omega_{Tj}^2 - \omega^2 - i\omega\Gamma_j},$$

where ε_∞ is the high frequency dielectric constant. The parameters ω_{Tj} and ω_{Lj} are the transverse (resonance) and longitudinal frequencies of the j-th oscillator. The Γ_j is the damping

constant. Two oscillators are assumed for the calculation. The measured spectrum is normalized to the calculated reflectivity at their peaks. The agreement is fairly good.

In Fig. 2 is shown reflection spectrum (solid curve) for the *E//b* polarization at 10 K. The reflection bands A and B are shifted to the high energy side by about 5 cm^{-1}, as compared with those at RT (Fig. 1). The intensities of the bands become larger and the widths become narrower as temperature is lowered. The third band labelled C is recognized at 238 cm^{-1} as a shoulder of the B band. Tha calculated spectrum (broken curve) was obtained by assuming three oscillators in the energy range shown. The LO phonon energies used in the calculation are 256 and 247 cm^{-1} for the B and C bands. These are in rough agreement with the energies of the scattering lines 260 and 252 cm^{-1} obtained from the RR experiments. In the RR spectrum, the intensity ratio of the sacttering line of 260 cm^{-1} to that of 252 cm^{-1} is about 2,[1] so that ratio of the oscillator strength of the phonon modes corresponding to the B and C bands was assumed to be 2 in the calculation. The calculated spectrum well reproduces the observed spectrum. Thus it is considered that two LO phonons with nearly equal energies of about 260 cm^{-1} are resolved also in the infrared reflection spectrum at low temperatures.

References

1) O. Arimoto, H. Takeuchi, and K. Nakamura: to be appeared in Phys. Rev. B**46** (1992).
2) H. Sobotta, H. Neumann, N.N. Syrbu, and V. Riede: Phys. Status Solidi (b)**115** (1983) K55.

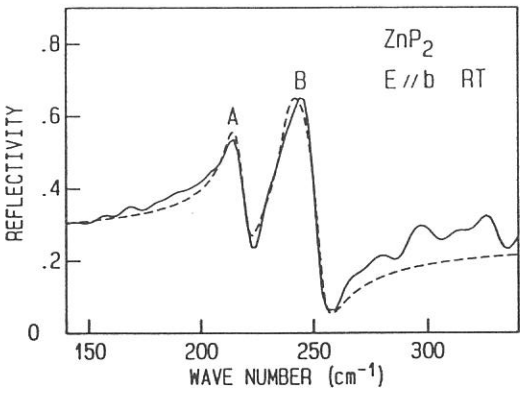

Fig.1. Reflection spectrum for *E//b* at RT.

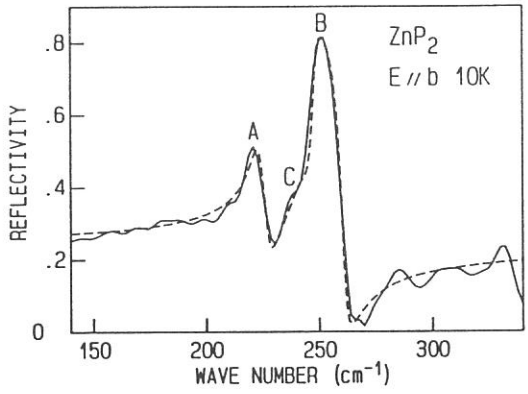

Fig.2. Reflection spectrum for *E//b* at 10 K.

Optical Phonon in YbB_6

S. Kimura, T. Nanba[+], S. Kunii[++] and T. Kasuya[++]
Research Institute for Scientific Measurements, Tohoku University, Aoba-ku, Sendai 980
[+]Department of Physics, Faculty of Science, Kobe University, Nada-ku, Kobe 657
[++]Department of Physics, Faculty of Science, Tohoku University, Aoba-ku, Sendai 980

Almost all rare-earth hexaborides (RB_6's) behave like monovalent metals because the rare-earth ion is trivalent and the valence of B_6 molecule is -2. On the other hand, however, YbB_6 becomes a narrow-gap semiconductor due to Yb^{2+} ion in YbB_6. Therefore the infrared active phonon modes, which are not seen in trivalent RB_6, are expected to be observed in YbB_6 because a strong Drude absorption which is seen in trivalent RB_6 may be much reduced due to very low concentration of conduction electron in YbB_6. Now, we measured the reflectivity spectrum of YbB_6 in the photon energy range from 1 meV to 40 eV at 300 K and 9 K for the purpose of obtaining the information of infrared active phonons.

The reflectivity was measured in the photon energy range from 1 meV to 40 eV. In the far-infrared region from 1 meV to 30 meV, the measurement was done by two different methods. One is by using the beam line BL6A1 of UVSOR and the other using a normal far-infrared spectrophotometer system. The same reflectivity spectrum was obtained by both methods.

YbB_6 becomes a narrow gap semiconductor ideally as mentioned above. However this material actually has a few number of conduction electrons because of the defect of Yb ion. This fact was seen in the reflectivity spectrum in Fig. 1. The Drude like reflectivity spectrum was observed in the energy range below 0.2 eV. From the fitting of the Drude model, the effective number of conduction electron was estimated to be 0.87 % / f. u. at 300 K and 0.96 % / f. u. at 9 K. The result of the weak temperature dependence is consistent with the result of the Hall effect qualitatively [1]. In the spectrum, two definite peaks indicated by A and B were observed. These peaks are discussed below.

From the Kramers-Kronig transformation of the reflectivity spectrum, we obtained the imaginary part of the dielectric constant (ε_2). Fig. 2 shows the ε_2 spectra of peaks A and B. Both of the peaks show simple Lorentzian shapes.

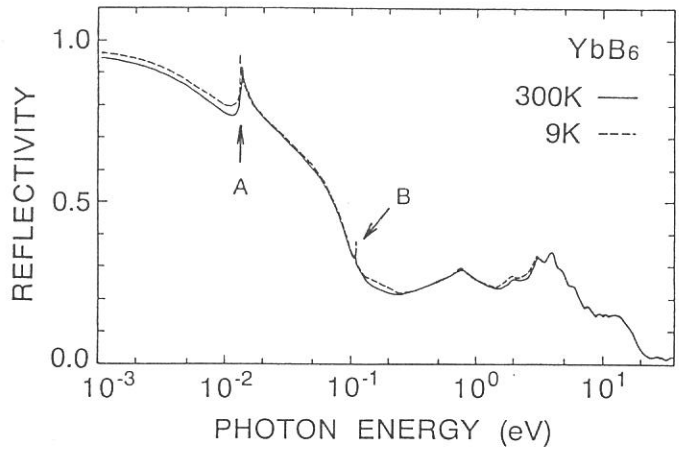

Fig. 1 Reflectivity spectrum of YbB_6 in the photon energy range from 1 meV to 40 eV at 300 K and 9 K. The peaks indicated by A and B are two kinds of optical phonons.

The phonon dispersion curve of YbB_6 was calculated by Takegahara *et al.* [2] According to the calculation result, the phonon energies of two kinds of t_{1u}–modes at Γ–point of Brillouin zone were given as 18 meV and 108 meV. These theoretical values agree with the experimental results qualitatively. Therefore it was seen that the peak A was the mode due to the relative motion between Yb and B_6 and the peak B an intra–molecular vibration in B_6. These two kinds of t_{1u}–modes are shown in Fig. 3 schematically. For the peak B, the experimentally obtained phonon energy was quite indicated to the theoretical value which reproduced the result of Raman measurement. On the other hand, however, the energy position of the peak A was about 30 % lower than that of the calculation. This means that the actual second derivative of the binding energy between Yb and B_6 is smaller than that estimated in the calculation. Since the bottom of conduction band consists of bonding states between Yb–$5d(e_g)$ and B_6–$2p(t_{2u})$, the hybridization between these states is considered to give an influence to the binding energy between Yb and B_6.

References

[1] J. M. Tarascon, J. Etourneau, P. Dordor, P. Hagenmuller, M. Kasaya and J. M. Coey, J. Appl. Phys. **51** (1980) 574.

[2] K. Takegahara and T. Kasuya, Solid State Commun. **53** (1985) 21.

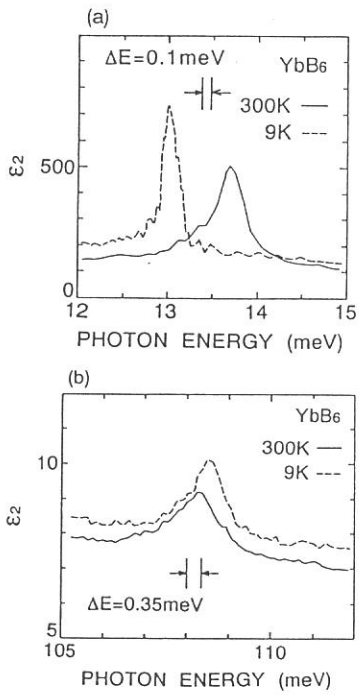

Fig. 2 Imaginary part of dielectric constant (ε_2) of two kinds of phonon absorption structures at 300 K and 9 K; (a) is for the peak A at about 13 meV. This peak is assigned to be due to the t_{1u}–mode between Yb and B_6. (b) is for the peak B at about 108 meV which is assigned to be due to the t_{1u}–mode in B_6–octahedron.

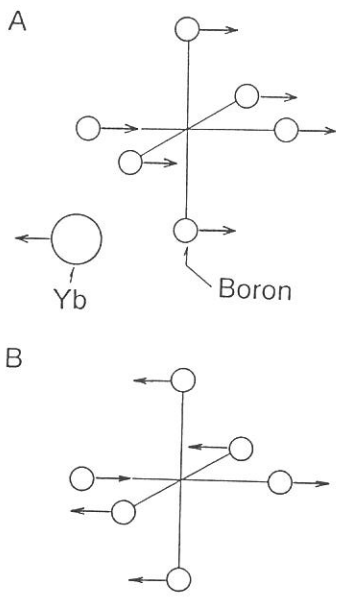

Fig. 3 Schematic pictures of two kinds of t_{1u}–modes of infrared active phonon. A is the mode between Yb and B_6 and B is the mode of intra B_6–octahedron.

IONIC PLASMON IN SUPERIONIC COPPER CONDUCTOR

Teruyoshi AWANO, Takao NANBA* and Mikihiko IKEZAWA**

Department of Applied Physics, Tohoku Gakuin University, Tagajo 985
*Department of Physics, Kobe University, Kobe 657
**Research Institute for Scientific Measurements, Tohoku University, Sendai 980

We have studied ionic motion in superionic conductors, which have very high ionic conductivity at solid phase. Absorption structure due to translational motion of mobile ions is expected to appear at the spectral range less than a few tens wave numbers considering from the mass of conduction ion and the potential barrier for conduction ion. The brilliance of the UVSOR light in this spectral region made it possible to measure the reflectivity or absorption spectra of small superionic crystals precisely. We had measured reflectivity spectra of some silver ion conductors of the form of MAg_4I_5 (M=Rb, K and NH_4). Shoulder peaks in energy loss function (imaginary part of dielectric constant) were observed in the spectral region below 10 cm^{-1} in these crystals. We have assigned these peaks as being due to ionic plasma oscillation.[1] In this work we have investigated copper ion conductors $Rb_4Cu_{16}Cl_{13}I_7$ and Cu_2HgI_4 to compare the plasma frequency with that of silver ion conductors. The former crystal has the same structure as MAg_4I_5 and has the highest ionic conductivity among all of the superionic conductors at room temperature. It is expected that the plasma frequency is proportional to the inverse of the root of the mass of conduction ion.

Reflectivity spectra were measured and transformed into optical constants by Kramers-Kronig analysis.

Fig. 1 shows conductivity spectra of $Rb_4Cu_{16}Cl_{13}I_7$ obtained from the reflectivity spectra. One peak near 40 cm^{-1} at 300 K split into two peaks at 15 K. This peaks seems to be due to the attempt vibration of copper ion in the cage of iodine ions and chlorine ions. The splitting seems to be due to the different shape of the potential cage by iodine ion from that by chlorine ion. The shoulder on the low energy side of this 40 cm^{-1} peak grows when the temperature rises. This phenomenon was observed also in the case of MAg_4I_5 and be due to translational motion of conduction ions. Fig. 2 shows energy loss function spectra obtained from the reflectivity spectra. The dashed and dotted curves show calculated one by the ionic Drude model. Parameters of curve fitting are listed in table 1. The agreement is good at 300 K although it is not good at 150 K. The cooperative motion which is noted as "ionic plasmon" seems to be impossible at low temperature because of strong scattering by immobile ions. Increase of dielectric constant at high energy side (ε_∞) seems to be due to the relative increase of vibrational motion of ions. Obtained plasma frequency is in good agreement with that estimated from mass and number of conduction ions.

Fig. 3 shows energy loss function of Cu_2HgI_4. The transition temperature to the superionic phase is 340 K. These shoulders disappeared at 77 K. As shown in table 1. plasma frequency is almost the same as that of $Rb_4Cu_{16}Cl_{13}I_7$. Small difference of ω_γ and ε_∞ from those of $Rb_4Cu_{16}Cl_{13}I_7$ seems to be due to the difference of potential barriers and the number of conduction ion in both crystal.

1) T.Awano, T. Nanba and M. Ikezawa, Solid State Ionics, 53-56 (1992) 1269

Table 1. Parameters in the Drude curve fitting.

$Rb_4Cu_{16}Cl_{13}I_7$	Temp. (K)	ω_p (cm^{-1})	ω_γ (cm^{-1})	ε_∞
	300	42	75	10
	230	42	85	11
	150	40	95	13
Cu_2HgI_4	Temp. (K)	ω_p (cm^{-1})	ω_γ (cm^{-1})	ε_∞
	320	49	95	8
	300	53	110	9

Fig. 1. Conductivity spectra of $Rb_4Cu_{16}Cl_{13}I_7$.

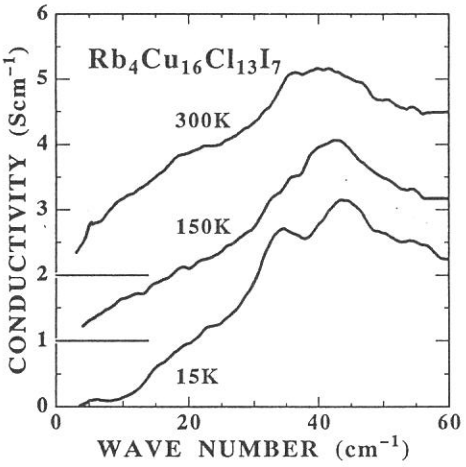

Fig. 2. Energy loss function spectra of $Rb_4Cu_{16}Cl_{13}I_7$.

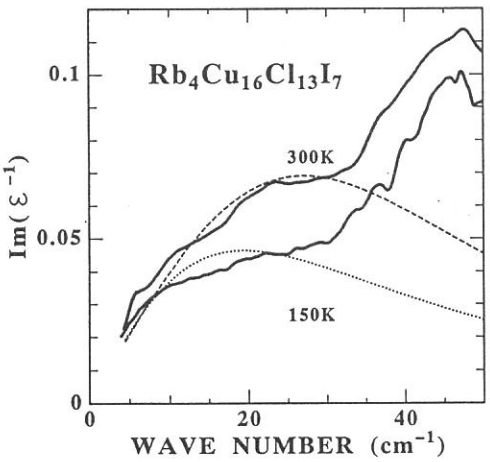

Fig. 3. Energy loss function spectra of Cu_2HgI_4.

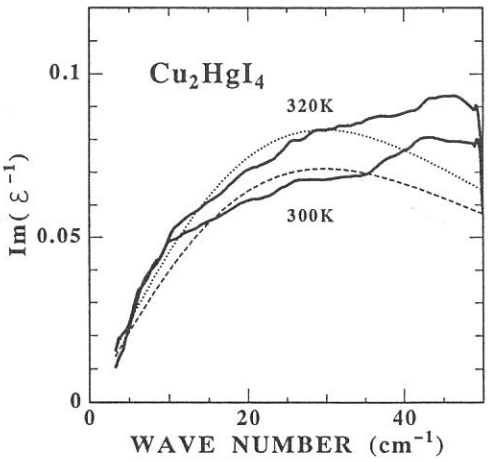

Far Infrared Absorption of NaCl Microcrystal under Pressure

T.Nanba,T.Matsuya and M.Motokawa

Department of Physics, Faculty of Science, Kobe University, Nada-ku, Kobe 657

The far infrared absorption spectrum of the NaCl microcrystal was measured at room temperature. As the crystal size decreases to a microcrystal, a so-called surface phonon mode can be induced because of the important role of the atoms which exist at the surface. The absorption due to such surface phonon mode under atmospheric pressure is known to be very sensitive to the shape and the size of the microcrystal. Such phenomena has been well explained by the continuum theory [1]. The purpose of the present study is to make clear the behavior of the surface phonon mode of the microcrystal under pressure.

The spherical NaCl microcrystal was obtained by a conventional gas evaporation techniques and its shape and size distribution were determined by an electron microscopic observation. The average size of microcrystals was 0.5-2 um. On the other hand , the cubic-shaped NaCl microcrystal was obtained by griding of the bulk NaCl down to the powders. The size distribution was also confirmed to be 1-3 um by the electron microscopic method. The sizes of both spherical and cubic samples are much smaller than the far infrared wavelength (40-400 um). A small amount of microcrystals were mixed with a transparent medium (apiezon grease-N) in the far infrared region and enclosed in the diamond anvil cell for the transmission measurement under high pressure at the BL6A1 of the UVSOR.

Observed peak positions of the absorption due to the surface phonon of the microcrystals were plotted as the function of the applied pressure to the sample and shown in Fig.1 in comparison with the peak positions of those absorption due to the bulk TO phonon mode of NaCl which were measured independently with thin films. We found that the energies of the surface phonons are quite different even at P=0 between a spherical (denoted as the "spherical" in the figure) and a cubic-like microcrystal (the "cubic").

According to the continuum theory [1], the surface phonon mode of the microcrystal in the spherical shape occurs at the frequency (ωs) which fills the equation

$$\varepsilon(\omega s) = -2 * \varepsilon m .$$

Here, ε is the dielectric function of the material comprising the sphere and εm the dispersionless dielectric constant of the medium surrounding the sphere. Similar theory was developed to the case of the cubic-shaped microcrystal by Fuchs [2] and he obtained that the energy of the dominant surface phonon mode in the the cubic microcrystal is given by the equation of

$$\varepsilon(\omega s) = -3.68 * \varepsilon m.$$

The difference in the surface phonon energies of the microcrystals in both shapes seen at P=0 in the figure can be explained by considering the difference in these two conditions. The phonon modes of all samples showed a blue shift with the applied pressure and the pressure dependences are different each other. We extended the above continuum model which has been developed only at P=0 to the case of the microcrystals under high pressure and revealed that the difference in the pressure dependence of the phonon energies of the microcrystal on its shape can be explained if we consider the increase of the dielectric constant of the surrounding medium with the pressure.

References

[1] L.Genzel and T.P.Martin: Surface Science **34**(1973) 33.
[2] R.Fuchs: Phys.Rev.**B11**(1975)1732.

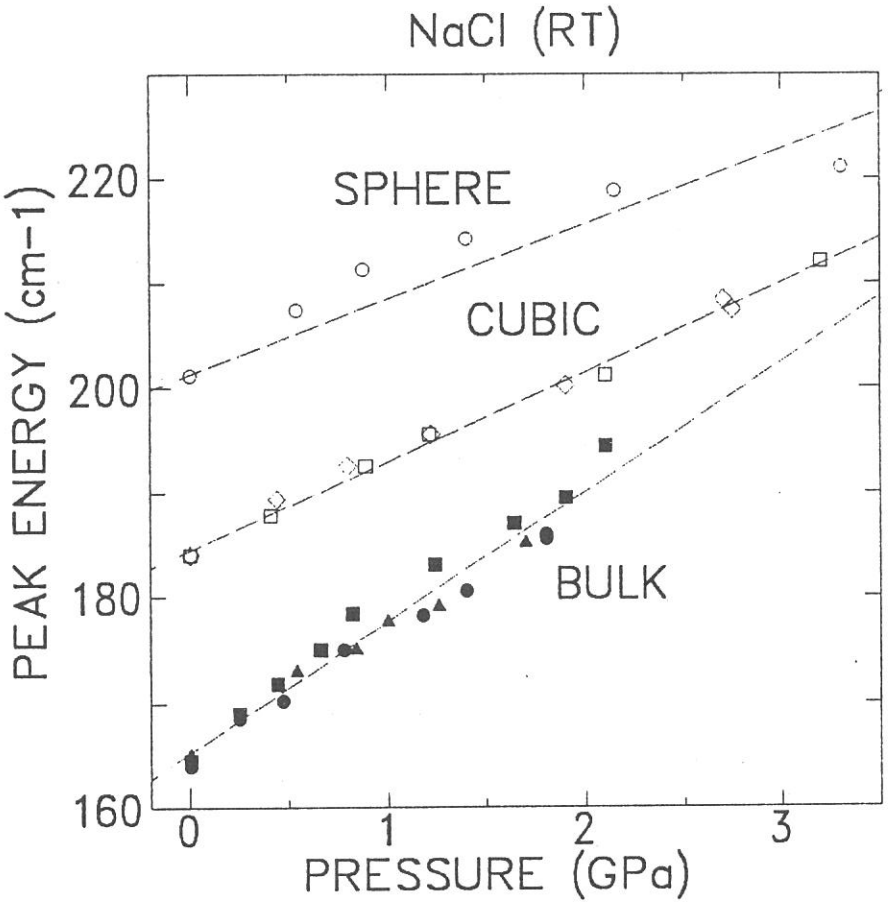

Fig.1
Pressure dependences of the peak positions of the absorption bands due to the surface phonon modes of the microcrystals in the different shapes with the applied pressure. The names of "SPHERE", "CUBIC" and "BULK" in each curve correspond to the shape of the microcrystals,respectively.

PROTON ORDER-DISORDER PHASE TRANSITION IN HIGH PRESSURE PHASE OF ICE OBSERVED BY VIBRATIONAL SPECTRA

M. KOBAYASHI, T. NAKAI, T. NANBA* and M. KAMADA

Faculty of Engineering Science, Osaka University, Toyonaka, Osaka 560
*Department of Science, Kobe University, Rokkodai, Kobe 657
Institute for Molecular Science, Myodaiji, Okazaki 444

Recently we reported far-infrared absorption spectra of high pressure phases in ice for the first time by using a diamond anvil cell and the synchrotron radiation [1]. We have extended the measurements by changing sample thickness in order to determine more precise spectral shapes.

Ice VII and VIII have almost the same atomic structure regarding arrangements of oxygen ions, while protons in VII and VIII have disordered and ordered structures, respectively. Figure 1 shows the absorption spectra of H_2O and D_2O ice in VII and VIII phases. In ice VII a broad absorption band whose peak locates at 140 cm^{-1} is observed. We designate this band as A. The band A disappears completely in ice VIII. Our former data showed that a weak absorption band still remains near at 120 cm^{-1} in ice VIII (cf. Fig. 1 of ref. [1]). This absorption turned out, however, to be only apparent arising from the Fabry-Perot interference between both the sides of sample, since the peak position changes depending on the sample thickness, and when we used thick enough sample, the absorption disappeared. On the other hand, another absorption band whose peak locates at 200 cm^{-1} appears in ice VIII at 3 GPa. We designate this band as B.

We measured pressure dependence of the spectra in ice VIII. Figure 2 plots the pressure dependence of the center position of the band B. When we assume a linear relation between the energy and the pressure, it gives a pressure coefficient of 18.2 cm^{-1}/GPa. When the relationship is extrapolated to the zero pressure, the energy of the band B becomes 153 cm^{-1}. This value is comparable to 162 cm^{-1}, which was obtained in pressure quenched sample of ice VIII by Tay et al. [2] and ascribed to the translational mode $\nu_T E_u$ [2]. Taking into consideration of the restricted numbers of experimental points and the experimental error, we conclude that the band B is ascribed to $\nu_T E_u$ mode. Our measurements correspond to the in situ observation of $\nu_T E_u$ mode at high pressures. The pressure quench is impossible for ice VII. Therefore, the in situ observation is indispensable to elucidate the effect

of proton ordering, because one should compare the spectra for both the phases at high pressure.

The band A in ice Ⅶ is ascribed to the absorption induced by random motion of protons. Ice Ⅶ and Ⅷ have almost the same lattice constants and densities. Therefore, both the phases show common elastic characteristics. Since the atomic arrangements of oxygen ions are almost invariable during the Ⅶ – Ⅷ transition, the Brillouin zone itself is definite in ice Ⅶ. The random motion of protons in ice Ⅶ breaks, however, the translational symmetry, which results in the non-conservation of the crystal momentum. Thus the whole phonon branches become optically active and therefore the absorption spectra reflects the density of states [3]. The peak A is presumably ascribed to the maximum of the density of states corresponding to the zone boundaries.

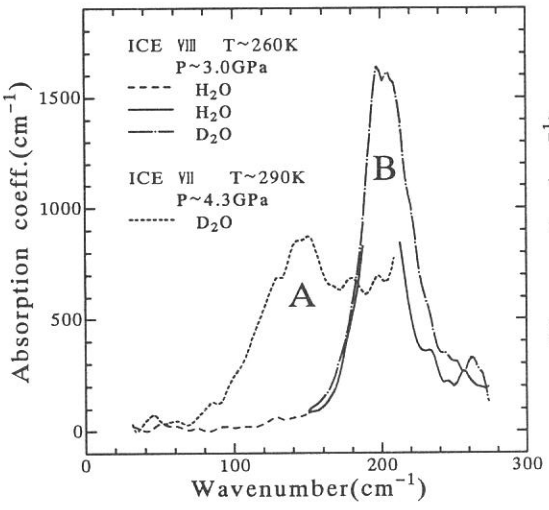

Fig.1 Far-infrared absorption spectra of ice Ⅶ and Ⅷ at high pressures.

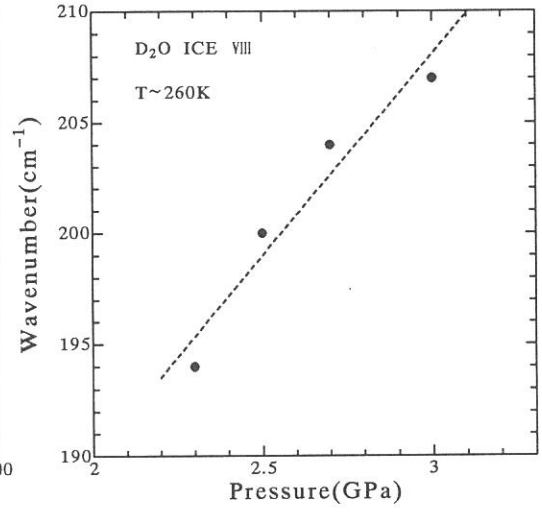

Fig.2 Pressure dependence of the energy of band B in ice Ⅷ.

REFERENCES

[1]M. Kobayashi, S. Morita, T. Nakai, T. Nanba and M. Kamada, UVSOR Activity Rep. (1991) 62.

[2] S. P. Tay, D. D. Klug and E. Whalley, J. Chem. Phys. 83 (1985) 2708.

[3] E. Whalley and J. E. Bertie, J. Chem. Phys. 46 (1967) 1264.

Far-infrared absorption of non-polar liquids and liquid C_6H_6 - C_6F_6 mixtures

Yoshitaka FUJITA and Shun-ichi IKAWA

Department of Chemistry, Faculty of Science, Hokkaido University, Sapporo 060

Previously, we measured the far-infrared collision-induced absorption(CIA) of liquid CS_2, CCl_4, C_6H_6 and C_6F_6 under pressure and observed that average induced dipole moments of the system $\sqrt{\langle\mu^2\rangle}$ obtained from the zeroth moment of the CIA bands decreased with increasing pressure, while the second moments M_2 increased[1]. In this study the CIA bands of liquid C_6H_6, C_6F_6 and $C_6H_3F_3$ have been measured in the pressure ranges 1 to 1250 bar, 540 bar and 890 bar, respectively, to further confirm the pressure dependence of $\sqrt{\langle\mu^2\rangle}$. In addition, we have measured liquid mixture of C_6H_6 and C_6F_6 at temperatures in the 13 ~ 45 °C range.

The high-pressure cell and the method of the analysis were described previously[1),2)]. For measurements of the liquid mixtures at ambient pressure, a liquid cell with Si windows of 3mm and 4mm thicknesses was used, and the sample thicknesses were 2 ~ 6.5mm. Fig.1 shows the resulting $\sqrt{\langle\mu^2\rangle}$ and M_2 plotted against pressure with the results for CS_2 and CCl_4. Obviously $\sqrt{\langle\mu^2\rangle}$ decrease while M_2 increase with increasing pressure, and freezing strengthens this tendency. Recently we have carried out the molecular dynamics simulation of liquid CS_2 at higher pressures and found the similar decrease in $\sqrt{\langle\mu^2\rangle}$ near the pressure of freezing, which is due to increase in the intermolecular correlation of the induced dipole moments.

Fig.2 shows the observed spectra of the equimolar mixture of C_6H_6 and C_6F_6. All the spectra of the mixture were measured with an InSb detecter and $\sqrt{\langle\mu^2\rangle}$ were obtained from the curves fitted to the spectral densities $\alpha(\nu) / \nu^2$ using a

function $1/(a+bv^2+cv^4+dv^6)$. The resulting $\sqrt{\langle\mu^2\rangle}$ values plotted against temperature are shown in fig.3. The large value of $\sqrt{\langle\mu^2\rangle}$ for the solid phase indicates the strong interaction between these two molecules[3].

References

1) Y.Fujita, T.Cho and S.Ikawa, UVSOR Activity Report 1991, p84.

2) Y.Fujita, T.Oba and S.Ikawa, Can.J.Chem.,69,1745(1991).

3) C.S.Patrick and G.S.Prosser, Nature 187.1021(1960).

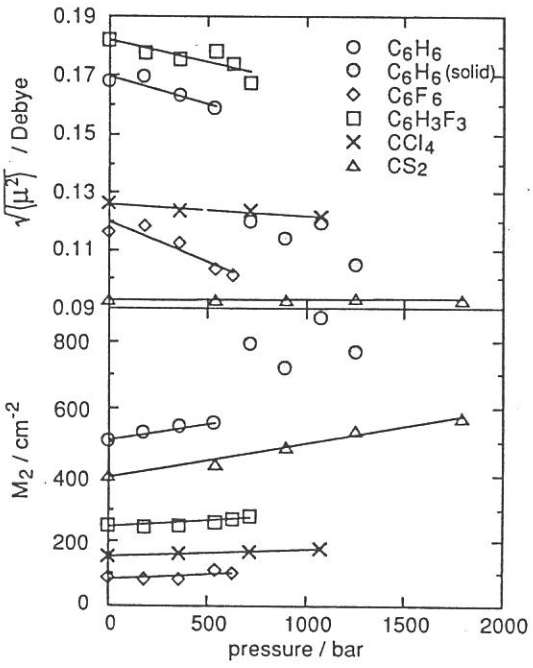

Fig. 1 $\sqrt{\langle\mu^2\rangle}$ and $M_2 = \int \alpha(\nu)\, d\nu$ of liquid CS_2, CCl_4, C_6H_6, C_6F_6 and $C_6H_3F_3$ plotted against pressure.

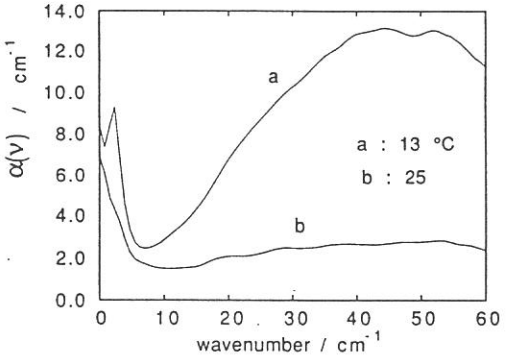

Fig. 2 Far-infrared spectra of the equimolar mixture of C_6H_6 and C_6F_6.

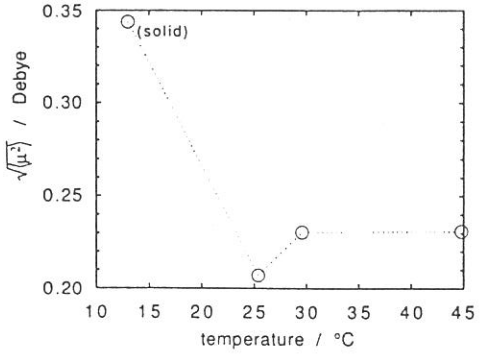

Fig. 3 $\sqrt{\langle\mu^2\rangle}$ plotted against temperature.